

# N=4 SYM model for soft interactions at high energy

---

**E. Levin<sup>a,b</sup> and I. Potashnikova<sup>b</sup>**

*a) Department of Particle Physics, School of Physics and Astronomy,  
Raymond and Beverly Sackler Faculty of Exact Science, Tel Aviv University, Tel Aviv, 69978, Israel*

*b) Departamento de Física, Centro de Estudios Subatómicos, Universidad Técnica Federico Santa  
María, and Centro Científico-Tecnológico de Valparaíso, Casilla 110-V, Valparaíso, Chile*

**ABSTRACT:** In this paper we compare the prediction for high energy soft interactions in the model of  $N = 4$  SYM, with the experimental data. It is shown that this model is able to describe the total, elastic and inelastic cross sections and the elastic slope with only three free parameters. However, the model failed to obtain the cross sections for diffractive production, which was close to the experimental data, giving small values for them. We believe that the theory of  $N = 4$  SYM, of the order of  $1/\lambda$  is needed to find the origin of large mass diffraction.

**KEYWORDS:** N=4 SYM, graviton reggeization, eikonal approach.

---

## Contents

<b>1. Introduction</b>	<b>1</b>
<b>2. Main formulae for high energy scattering amplitude in <math>N=4</math> SYM</b>	<b>2</b>
2.1 Reggeized graviton(Pomeron) propagator	2
2.2 Vertices for Pomeron interaction with colliding hadrons	4
2.3 Eikonal formula	5
2.4 Nucleon-nucleon scattering at high energy: observables	5
2.5 Proton wave function	6
<b>3. Description of the experimental data</b>	<b>6</b>
3.1 Fitting parameters	6
3.2 The result of the fit	7
3.3 Comparison with the LHC data	9
3.4 Survival probability of large rapidity gaps	10
<b>4. Conclusions</b>	<b>11</b>

---

## 1. Introduction

It turns out that all soft interaction models [1, 2, 3, 4] have failed to predict the new LHC data (see Refs. [5, 6, 7, 8]), showing that our understanding of long distance physics is very limited (if any). With this in mind it seems reasonable to us, to build a model for high energy strong interactions, based on  $N = 4$  SYM, which is the only theory capable of treating long distance physics.  $N = 4$  SYM is a unique theory which allows us to study theoretically, the regime of the strong coupling constant [9].

Therefore in principle, comparing the prediction for the high energy scattering amplitude in  $N = 4$  SYM with the experimental data, we can single out the physics phenomena described by QCD more successfully than this simplified approach. It is well known (see for example Refs. [11, 12, 16, 17, 18] and references therein\*) that the main small parameters of  $N = 4$  SYM are

---

\*We select here only those references which are related to the high energy scattering amplitude in  $N = 4$  SYM, which will be useful for an understanding of this paper.

$$\lambda \gg 1 \left( \rho \equiv \frac{2}{\sqrt{\lambda}} \ll 1 \right) \text{ but } g_s \ll 1 \quad (1.1)$$

where

$$\lambda = 4\pi N_c g_{YM}^2; \quad g_s = \frac{g_{YM}^2}{4\pi}; \quad L = \alpha'^{\frac{1}{2}} \lambda^{\frac{1}{4}}; \quad (1.2)$$

and  $g_s$  is the string constant,  $\alpha' \approx 1 \text{ GeV}^{-2}$  is the slope of the reggeon trajectory,  $N_c > 1$  is the number of colours, and  $L$  is the radius of  $\text{AdS}_5$  space.

As shown in our previous paper [10], the theory of  $N = 4$  SYM in which  $\rho$  is small (say  $\leq 0.25$ ), could be responsible for a small part of the total cross section, for energies below the LHC energy range. In this paper we build an  $N = 4$  SYM model based on the classical understanding of this word: a model is the theory which we apply in the kinematic region where the theory can't be proved to be incorrect. We expand the theory of  $N = 4$  SYM developed for  $\rho \ll 1$ , up to arbitrary values of  $\rho$ .

Comparing with the experimental data, we find the value of  $\rho$  to be  $0.7 \div 0.8$ . We are able to describe the experimental data on the total, inelastic and elastic cross sections in the entire range of energies, including the LHC range. However, we failed to describe the values and energy behaviour for diffractive production. We conclude from this failure, that we need to include high mass diffractive production which traditionally stems from the triple Pomeron interaction. This interaction has not appeared in  $N = 4$  SYM for small  $\rho$ . Therefore, we need to find the  $\rho^2$ -corrections, in order to treat diffractive production in  $N = 4$  SYM.

## 2. Main formulae for high energy scattering amplitude in N=4 SYM

### 2.1 Reggeized graviton(Pomeron) propagator

Before discussing the general approach of  $N = 4$  SYM to high energy scattering, we would like to draw the reader's attention to the fact that there exists two different regions of energy, that we have to consider in  $N = 4$  SYM:  $\rho\alpha's < 1$  and  $\rho\alpha's > 1$  (see Eq. (1.2)). In the first region, the multiparticle production has a very small cross section, and it can be neglected. However, in the second region the graviton reggeization leads to the inelastic cross section that is rather large, and at ultra high energies the scattering amplitude reveals all of the typical features of the black disc regime:  $\sigma_{el} = \sigma_{in} = \sigma_{tot}/2$ .

At  $\rho \rightarrow \infty$  the main contribution to the scattering amplitude at high energy in  $N = 4$  SYM stems from the exchange of one graviton. The formula for this exchange has been written in Ref. [14, 16, 18]. In  $\text{AdS}_5 = \text{AdS}_{d+1}$  space this amplitude takes the following form:

$$A_{1GE}(s, b; z, z') = g^2 T_{\mu\nu}(p_1, p_2) G_{\mu\nu\mu'\nu'}(u) T_{\mu'\nu'}(p_1, p_2) \xrightarrow{s \gg \mu^2} g^2 s^2 z^2 z'^2 G_3(u) \quad (2.1)$$

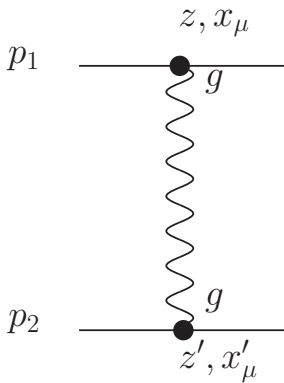


**Figure 1:** The one graviton (1GE) exchange.

and

$$G_3(u) = \frac{1}{4\pi} \frac{1}{\left\{1 + u + \sqrt{u(u+2)}\right\}^2 \sqrt{u(u+2)}} \quad (2.4)$$

where  $b$  is the impact parameter (see Fig. 1). As one can see from Eq. (2.1), the one graviton exchange amplitude is real and increases as  $s^2$ . However, the high energy limit of Eq. (2.1) has to be modified, since in the order of  $\rho$ , the intercept of the graviton decreases and becomes equal to  $2 - \rho$  (see Refs/ [13, 14, 15, 12, 16]). The resulting expression for Eq. (2.1) which we can consider to be the propagator of the reggeized graviton exchange, takes the following form:

$$A_{1GE}(s, b; z, z') \rightarrow P(s, b; z, z') = (\cot(\pi\rho/2) + i) \frac{\xi_0}{\sinh(\xi_0) \tau^{3/2} \sqrt{u(u+2)}} \exp\left((1-\rho)\tau - \frac{\xi_0^2}{\rho\tau}\right) \quad (2.5)$$

where

$$\tau = \ln(\rho z z' s/2) ; \quad \xi_0 = \ln\left(1 + u + \sqrt{u(2+u)}\right) ; \quad (2.6)$$

One can see that Eq. (2.5) does not describe the exchange of the Regge pole with the intercept  $(1 - \rho)$ , but it is similar to the contribution of the BFKL Pomeron which is responsible for high energy scattering in  $N = 4$  SYM, but at  $g_s \ll 1$ . Therefore, Eq. (2.5) gives an explicit example of AdS-CFT correspondence [9] which inherits all of the bad features of the BFKL Pomeron

[19].

Firstly, for large values of the impact parameters, Eq. (2.5) falls down only as a power of  $b$ , and such a decrease results in a power-like increase of the radius of interaction, in the direction which contradicts

where  $T_{\mu\nu}$  is the energy-momentum tensor, and  $G$  is the propagator of the massless graviton. The last expression in Eq. (2.1), reflects the fact that for high energies,  $T_{\mu\nu} = p_{1,\mu} p_{1,\nu}$  and at high energies the momentum transferred  $q^2 \rightarrow q_{\perp}^2$  which led to  $G_3(u)$  (see Refs. [14, 18]). In  $AdS_5$  the metric takes the following form

$$ds^2 = \frac{L^2}{z^2} \left( dz^2 + \sum_{i=1}^d dx_i^2 \right) = \frac{L^2}{z^2} (dz^2 + d\underline{x}^2) \quad (2.2)$$

where  $u$  is a new variable which is equal to

$$u = \frac{(z - z')^2 + (\underline{x} - \underline{x}')^2}{2 z z'} = \frac{(z - z')^2 + b^2}{2 z z'} \quad (2.3)$$

the Froissart theorem [20] (see Ref. [21]). The second characteristic property of Eq. (2.5), as well as the BFKL Pomeron, is the absence of the shrinkage of the diffractive peak for high energy scattering.

In principle, the shadowing corrections which should be large in our case since the amplitude of Eq. (2.5) increases with energy, can generate the effective shrinkage of the diffractive peak. However, we have decided to introduce some corrections to Eq. (2.5), namely,

$$P(s, b; z, z') \longrightarrow \hat{P}(s, b; z, z') \equiv P(s, b; z, z') e^{-\sqrt{2\rho\alpha'} b - \frac{b^2}{2a\alpha'\rho\tau}} \quad (2.7)$$

The first term in the exponent of Eq. (2.7) includes the minimal mass that appears in string theory, which  $N = 4$  is the limit at  $\rho \ll 1$ . The second one takes the following form in  $q$  representation:  $\exp(-q^2 (a\rho/2) \tau)$  and corresponds to the shrinkage of the diffraction peak, with the effective  $\alpha' = a\rho/2$ .

## 2.2 Vertices for Pomeron interaction with colliding hadrons

It's well known that the contribution of the Pomeron to the scattering amplitude takes the following form

$$A_{\mathbb{P}}(s, q; z, z') = g_{\mathbb{P}}^2(q) \hat{P}(s, q; z, z') = g_{\mathbb{P}}^2(q) \int d^2 b e^{i\vec{q}\vec{b}} \hat{P}(s, b; z, z') \quad (2.8)$$

where  $g(q)_{\mathbb{P}}$  are the vertices of the Pomeron-hadron interaction. The vertex for the interaction of the graviton with the hadron has been found in the soft wall model for confinement [22], that describes a number of different hadron characteristics [23]. It has the following form (see Ref. [24]):

$$g_{\mathbb{P}}(q_T; z) = 2g_{YM} H(q_T, z) = 2g_{YM} \Gamma(a+2) U(a, -1, 2\xi) = 2g_{YM} a(a+1) \int_0^1 dt t^{a-1} (1-x) e^{-2\xi t/(1-t)} \quad (2.9)$$

where  $U(a, -1, 2\xi)$  is Tricomi's (confluent hypergeometric) function [25] and

$$\xi = \kappa^2 z^2; \quad a = \frac{q_T^2}{8\kappa^2}; \quad q_T^2 = -t \leftarrow \text{momentum transferred by the Pomeron} \quad (2.10)$$

where  $\kappa$  is the dimensional parameter of the soft wall approach, and  $\kappa^2 = m^2/8$  where  $m$  is the nucleon mass (see Ref. [23] for more details). We replace the exact formula of Eq. (2.9) by the following approximate expression

$$g_{\mathbb{P}}(q_T; z) = 2g_{YM} \exp\left(-B(\xi) a\right) \text{ with } B(\xi) = 1 - C + U^{(1,0,0)}(0, -1, 2\xi) \quad (2.11)$$

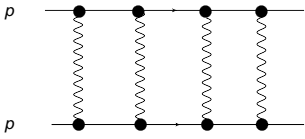
which allows us to perform analytically, part of the intergrations.  $C$  is the Euler constant in Eq. (2.11).

Finally, the amplitude for the exchange of a single Pomeron in impact parameter representation,

which we need in order to take into account the eikonal rescattering, has the form

$$\tilde{A}_{\mathcal{P}}(b, s; z, z') = \frac{1}{2\bar{B}} e^{-\frac{b^2}{4\bar{B}}} \int d^2b' I_0\left(\frac{\vec{b} \cdot \vec{b}'}{2\bar{B}}\right) \hat{P}(s, b; z, z') \quad (2.12)$$

### 2.3 Eikonal formula



As we have mentioned,  $A_{\mathcal{P}}(s, q; z, z')$  increases steeply with energy  $s$ , and has to be unitarized using the eikonal formula [14, 15, 12, 16, 18] (see Fig. 2)

**Figure 2:** The eikonal formula that takes into account the multi-Pomeron exchanges.

$$A_{eikonal}(s, b; z, z') = i \left( 1 - \exp\left(i \tilde{A}_{\mathcal{P}}(s, b; z, z' | Eq. (2.7))\right) \right) \quad (2.13)$$

In Ref. [13, 12] it was argued that AdS/CFT correspondence leads to the corrections to Eq. (2.13) which are small ( $\propto 2/\sqrt{\lambda}$ ). The unitarity constraints for Eq. (2.13) take the following form

$$2 \text{Im} \mathcal{A}_{eikonal}(s, b; z, z') = |\mathcal{A}_{eikonal}(s, b; z, z')|^2 + \mathcal{O}\left(\frac{2}{\sqrt{\lambda}}\right) \quad (2.14)$$

### 2.4 Nucleon-nucleon scattering at high energy: observables

We only need to integrate Eq. (2.13) with the wave functions of the proton, in order to obtain the amplitude for proton-proton scattering. Indeed the proton-proton amplitude is equal to

$$A_{pp}(s, b) = i \int dz dz' \Phi(z) \Phi(z') \left( 1 - \exp\left(i A_{\mathcal{P}}(s, b; z, z' | Eq. (2.7))\right) \right) \quad (2.15)$$

Based on Eq. (2.15), we can calculate the number of the experimental observable. We list below those of them that we actually use in our description.

$$\sigma_{tot} = 2 \int d^2b \int dz dz' \Phi(z) \Phi(z') \left(1 - \cos(\text{Re}A_{\mathcal{P}}) e^{-\text{Im}A_{\mathcal{P}}}\right); \quad (2.16)$$

$$\begin{aligned} \sigma_{el} = & \int d^2b \left( \left\{ \int dz dz' \Phi(z) \Phi(z') \left(1 - \cos(\text{Re}A_{\mathcal{P}}) e^{-\text{Im}A_{\mathcal{P}}}\right) \right\}^2 \right. \\ & \left. + \left\{ \int dz dz' \Phi(z) \Phi(z') \left(\sin(\text{Re}A_{\mathcal{P}}) e^{-\text{Im}A_{\mathcal{P}}}\right) \right\}^2 \right); \end{aligned} \quad (2.17)$$

$$\begin{aligned} \sigma_{sd} = & 2 \int d^2b \int dz \Phi(z) \left\{ \left( \int dz' \Phi(z') \left(1 - \cos(\text{Re}A_{\mathcal{P}}) e^{-\text{Im}A_{\mathcal{P}}}\right) \right)^2 \right. \\ & \left. + \left( \int dz' \Phi(z') \left(\sin(\text{Re}A_{\mathcal{P}}) e^{-\text{Im}A_{\mathcal{P}}}\right) \right)^2 \right\} \end{aligned} \quad (2.18)$$

$$\sigma_{dd} = \int d^2b \int dz dz' \Phi(z) \Phi(z') \left\{ \left(1 - \cos(\text{Re}A_{\mathcal{P}}) e^{-\text{Im}A_{\mathcal{P}}}\right)^2 + \left(\sin(\text{Re}A_{\mathcal{P}}) e^{-\text{Im}A_{\mathcal{P}}}\right) \right\} \quad (2.19)$$

$$B_{el} = \frac{\int b^2 d^b \int dz dz' \Phi(z) \Phi(z') \left(1 - \cos(\text{Re}A_{\mathcal{P}}) e^{-\text{Im}A_{\mathcal{P}}}\right)}{2 \int d^2b \int dz dz' \Phi(z) \Phi(z') \left(1 - \cos(\text{Re}A_{\mathcal{P}}) e^{-\text{Im}A_{\mathcal{P}}}\right)} \quad (2.20)$$

## 2.5 Proton wave function

The last ingredient of our approach is the wave function of the proton which we chose in the soft wall approximation [22]. It is given by:

$$\Phi(\xi_i) = \kappa \left( \frac{1}{\Gamma(5/2)} \xi_i^4 + \frac{1}{\Gamma(7/2)} \xi_i^6 \right) e^{-\xi_i^2} \quad (2.21)$$

This wave function works quite well for describing the key properties of the hadron, as shown in Refs. [23]. It is easy to see that

$$\int dz \Phi(z) = 1 \quad (2.22)$$

## 3. Description of the experimental data

### 3.1 Fitting parameters

As one can see our main formulae (see Eq. (2.7), Eq. (2.8), Eq. (2.11) and Eq. (2.13)) contain a number of parameters. We have fixed all of them except for three, from the description of the hadron characteristics in the soft wall model (see Refs. [22, 23]). These three fitting parameters are

$$g_s = \frac{g_{YM}^2}{4\pi}; \quad \rho = 2/\sqrt{\lambda}; \quad a \quad (3.1)$$

In  $N = 4$  SYM with AdS/CFT correspondence,  $g_s$  and  $\rho$  are much less than 1 while  $a = 0$ . In our model we consider them as free parameters that can have arbitrary values. The difference between the values of these parameters found from comparing our formulae with the experimental data, and the  $N = 4$  SYM expectations, will tell us how the  $N = 4$  SYM model differs from the theory. In principle, using the actual values of these three parameters, we can also estimate up to what order of magnitude in  $\rho^n$  we need to expand, in order to calculate the scattering amplitude, and to obtain a description of the experimental data.

### 3.2 The result of the fit

Using Eq. (2.7), Eq. (2.8), Eq. (2.11) and Eq. (2.13) we fit the experimental data starting with  $W = \sqrt{s} = 20 \text{ GeV}$ . We do not include the LHC data in the fit since we wish to check the predictive power of the model. Fig. 3 and Fig. 4 show the best result of our fit for  $\sigma_{tot}$ ,  $\sigma_{el}$  and the slope for  $d\sigma_{el}/dt$  at  $t = 0$ . The values of the parameters are  $g_s = 0.245 \pm 0.003$ ,  $\rho = 0.797 \pm 0.001$  and  $a = 0.23 \pm 0.005 \text{ GeV}^{-2}$ . The value of  $\chi^2/d.o.f. = 1.25$ , which is very good.

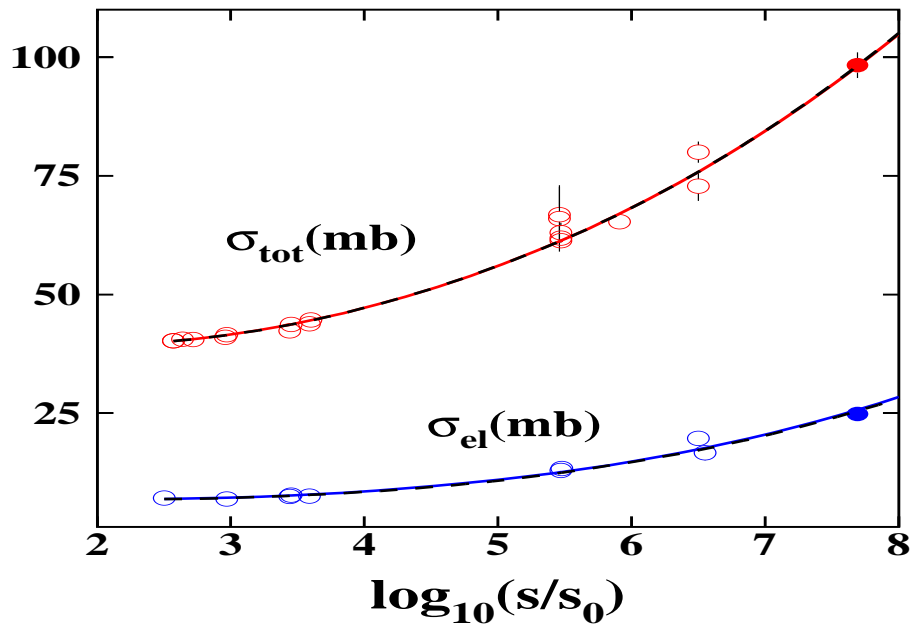


**Figure 3:** The description of the energy behaviour of the total and elastic cross sections with  $g_s = 0.245$ ,  $\rho = 0.797$  and  $a = 0.23 \text{ GeV}^{-2}$ . The solid line corresponds to the fit without the LHC data, while the dashed line describes the result of the fit that includes the LHC data. The open circles show the data from PDG [26], and the full circles show the LHC data [8].



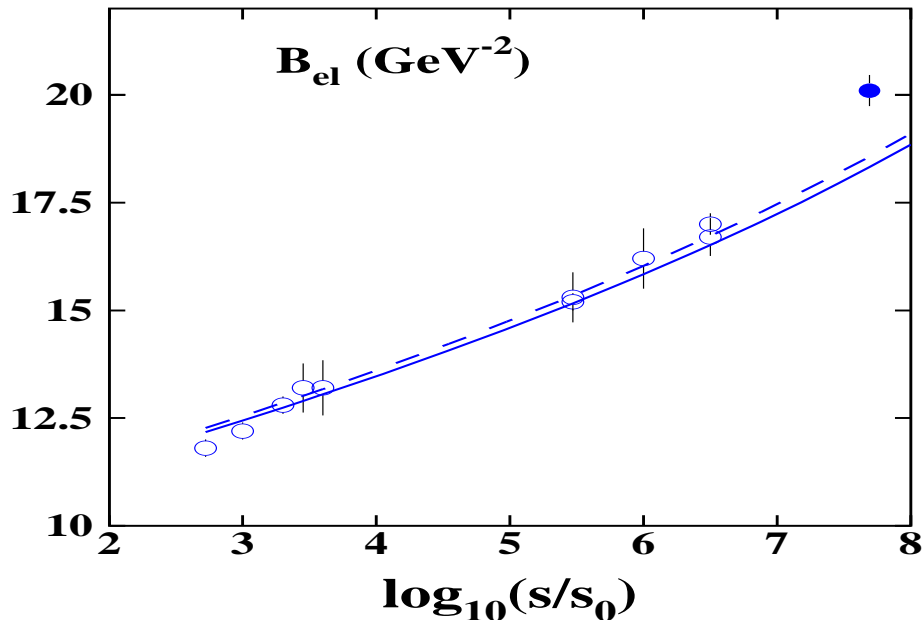


**Figure 4:** The description of the energy behaviour of the slope for the elastic cross section, with the same values of the parameters as in Fig. 3. The solid line corresponds to the fit without the LHC data, while the dashed line describes the result of the fit that includes the LHC data. The open circles show the data from PDG [26], and the full circles show the LHC data [8].

However, when we include the data for the diffractive cross section for either the single diffraction or the double diffraction, we failed to describe these sets of data. Our best values for these cross sections turn out to be less than 2 mb. Such values are in striking contradiction with the experimental data. For example at  $W = 7 \text{ TeV}$ , the values for the single diffractive cross section are as large as 14 mb. The reason why this happens is clear from Fig. 5. In these figures, we show the behaviour of  $\Phi(z)$ , as well as the real and imaginary parts of the scattering amplitude, as functions of  $z$ .

One can see that the amplitude depends only mildly on  $z$  in the region where  $\Phi(z)$  is not very small. Therefore, in Eq. (2.16)-Eq. (4) we can take the term for the amplitude outside of the integral at  $z = z_{max}$ , where  $z_{max}$  is the value of  $z$  where the function  $\Phi(z)$  has a maximum. In doing so, we obtain the result that the integral over  $z$  is equal to 1, and the cross sections for diffractive processes are equal to zero. At large  $b$ , the situation changes and the amplitude starts to depend on  $z$  in the region where  $\Phi(z)$  is not small. In this case we can see the difference in the integrals for elastic, single and double diffraction. Unfortunately, the region of large  $b$  gives only a small contribution.

The first conclusion from our fit, is that we need to find a new mechanism for diffractive processes. Actually, we know the missing ingredient in  $N = 4$  SYM. In the routine Pomeron approach, a substantial part of diffraction relates to the diffractive production of large masses, which stem from the triple Pomeron interaction (see Fig. 6-a). In our approach we do not have the triple graviton vertex. Therefore, we believe

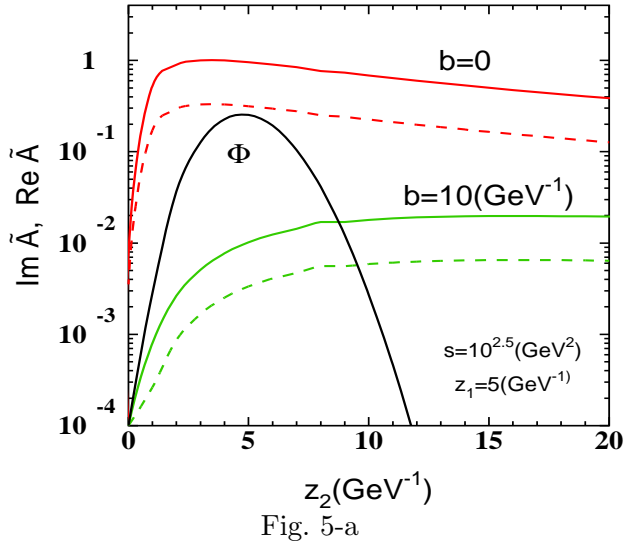


Fig. 5-a

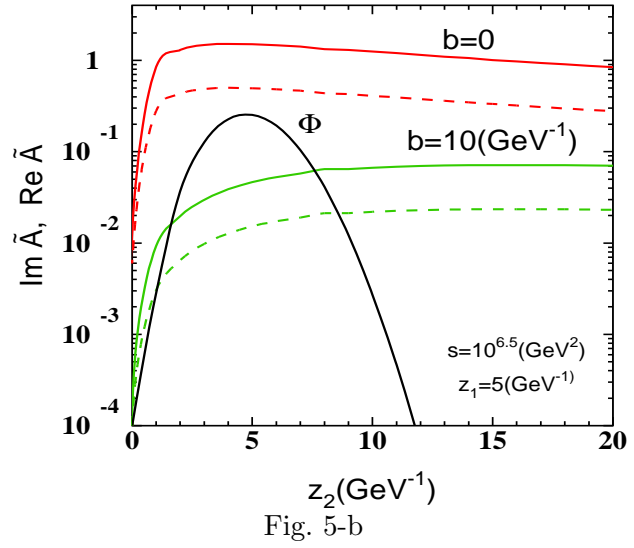


Fig. 5-b

**Figure 5:** The behaviour of the real (dotted line) and the imaginary (solid line) parts of the scattering amplitude, and  $\Phi(z)$  versus  $z$  for different energies:  $\log_{10}s = 2.5$  (Fig. 5-a) and  $\log_{10}s = 6.5$  (Fig. 5-b) and impact parameters ( $b$ ).

that we need to find up to what order of  $\rho^n$  in the expansion, this vertex appears in  $N = 4$  SYM. It should be stressed that in  $N = 4$  SYM with small coupling (weakly interacting  $N = 4$  SYM), the diffractive dissociation due to the triple BFKL Pomeron plays an essential role.

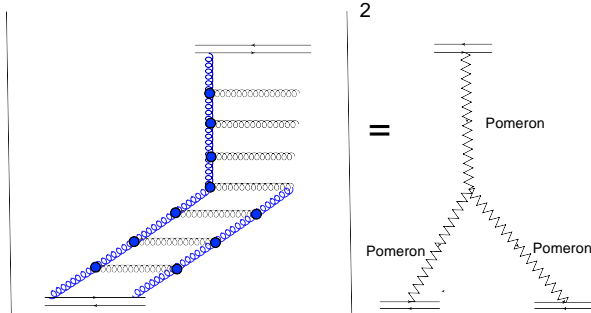


Fig. 6-a

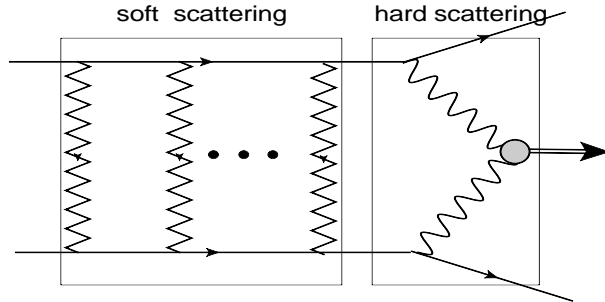


Fig. 6-b

**Figure 6:** The simple diagrams for large mass diffraction and its relationship with the triple Pomeron exchange in weakly coupled  $N = 4$  SYM (Fig. 6-a); and for central Higgs production (Fig. 6-b).

### 3.3 Comparison with the LHC data

Now let us consider the cross sections and other observables, within the LHC range of energies. As mentioned above we failed to describe the cross sections for single and double diffractive dissociation, obtaining extremely small values for both ( $\leq 2mb$ ). However, it turns out that the model can describe the data for the total, inelastic and elastic cross sections. The comparison of our model with the LHC data

W	$\sigma_{tot}^{model}$	$\sigma_{tot}^{exp}$	$\sigma_{el}^{model}$	$\sigma_{el}^{exp}$	Re /Im <sup>model</sup>
7 TeV	98.09 mb	TOTEM: $98.3 \pm 0.2^{st} \pm 2.8^{syst}$ mb	25.7 mb	TOTEM: $24.8 \pm 0.2^{st} \pm 1.2^{syst}$ mb	0.213
W	$\sigma_{in}^{model}$	$\sigma_{in}^{exp}$	$B_{el}^{model}$	$B_{el}^{exp}$	
7 TeV	72.4 mb	CMS: $68.0 \pm 2^{syst} \pm 2.2^{lumi} \pm 4^{extrap}$ mb ATLAS: $69.4 \pm 2.4^{exp} \pm 6.9^{extrap}$ mb ALICE: $72.7 \pm 1.1^{model} \pm 5.1^{extrap}$ mb TOTEM: $73.5 \pm 0.6^{st} \pm 1.8^{syst}$ mb	$18.3 \text{ GeV}^{-2}$	TOTEM: $20.1 \pm 0.2^{st} \pm 0.3^{syst} \text{ GeV}^{-2}$	

**Table 1:** The comparison of the prediction of our model with the experimental data at W=7 TeV.

is presented in Table 1. One can see that we predict the LHC data quite well, except for the value of the slope. In Fig. 7 we show the  $t$  dependence of the elastic cross section of our model, and the comparison of this distribution with the TOTEM experimental data. One can see that we overshoot the data, although the qualitative behaviour is reproduced quite well. We believe that to a large extent, our failure to describe the data is correlated with a sufficiently small slope that we have (see Table 1). The value of the ratio  $\text{Re}A/\text{Im}A$  that we obtain in the model, is larger than the value that uses TOTEM to extract the value of the total cross section ( $\text{Re}A/\text{Im}A = 0.14$  [27]), but the error coming from this difference, is well within the experimental error for the TOTEM value of the total cross section, namely,  $\sigma_{tot} = 96.8 \text{ mb}$ .

### 3.4 Survival probability of large rapidity gaps

For a long time it has been known that the cross section for processes with large rapidity gaps (for example central diffractive Higgs production (see Fig. 6-b)) has to be multiplied by a factor  $S^2$  which is called the survival probability [28, 29, 30]. This factor stems from the possible interaction of the constituents of the projectile, with the target that should be forbidden to preserve the gap. In other words, the constituents of the projectile could interact with the target in the initial or final state, suppressing the cross section for such processes (see Fig. 6-b). The straightforward generalization of the well known formulae [28, 29, 30] leads to the following expression for the survival probability  $S^2$ :

$$S^2 = \frac{\int d^2b \int dz dz' \Phi(z) \Phi(z') e^{-\text{Im}A_P(s,b;z,z')} A_{hard}^2(b)}{\int d^2b A_{hard}^2(b)} \quad (3.2)$$

where  $A_{hard}$  is the amplitude for Higgs production, in which the main contribution stems from short distances. One can see from Eq. (3.2) that the value for the survival probability depends on the impact parameter dependence, but not on the magnitude of the cross section. For simplicity we choose the exponential parametrization for  $A_{hard}^2(b)$ , namely,

$$A_{hard}^2 \propto \exp\left(-\frac{b^2}{2B}\right) \quad (3.3)$$

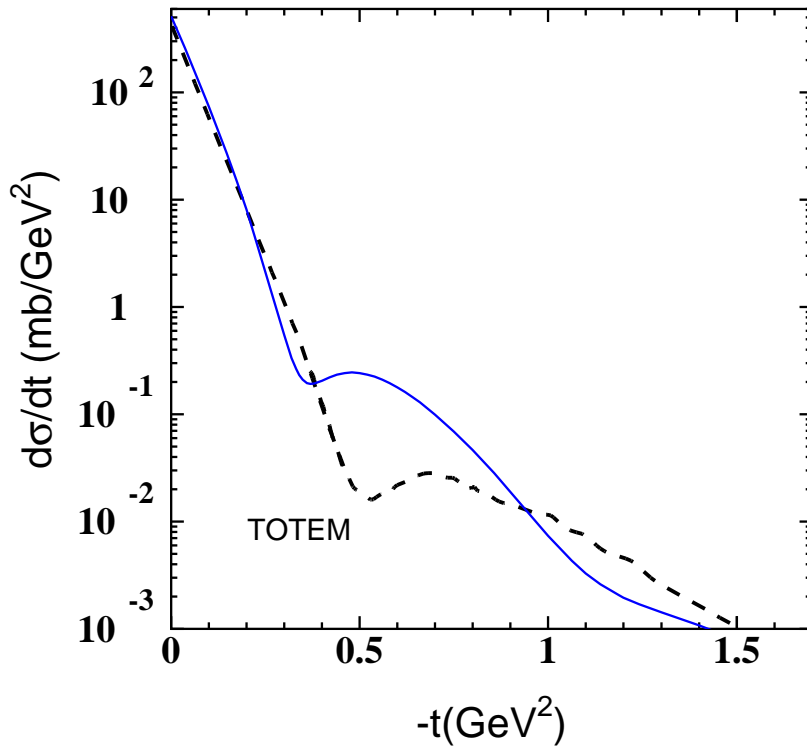


**Figure 7:**  $d\sigma_{el}/dt$  of our model (solid line), and the eye fit of the TOTEM experimental data ([8]) (dotted line).

where  $B$  is the slope of the hard differential cross section. In Fig. 8 which is taken from Ref. [33], the experimental values of the slope for DIS diffractive production are plotted.

From Fig. 8 we can conclude that the average  $B$  at large momentum scale (short distances), is about  $4 \div 5 \text{ GeV}^{-2}$ . We made estimates for  $S^2$  for two values of  $B$ :  $B = 4 \text{ GeV}^{-2}$  and  $B = 5 \text{ GeV}^{-2}$ , These estimates lead to the following values

$$\begin{aligned}
 B = 5 \text{ GeV}^{-2} &\longrightarrow \text{TEVATRON} : S^2 = 0.126; \quad \text{LHC} : S^2 = 0.084; \\
 B = 4 \text{ GeV}^{-2} &\longrightarrow \text{TEVATRON} : S^2 = 0.106; \quad \text{LHC} : S^2 = 0.068
 \end{aligned}
 \tag{3.4}$$

One can see that we obtain the value for  $S^2$ , which is  $2 \div 3$  times larger than all previous estimates [31, 32].

#### 4. Conclusions

In this paper we showed that the model of  $N = 4$  SYM is able to describe the experimental data for the total, elastic and inelastic cross sections, and on the elastic slope in the range of energies from  $W = 20 \text{ GeV}$ ,

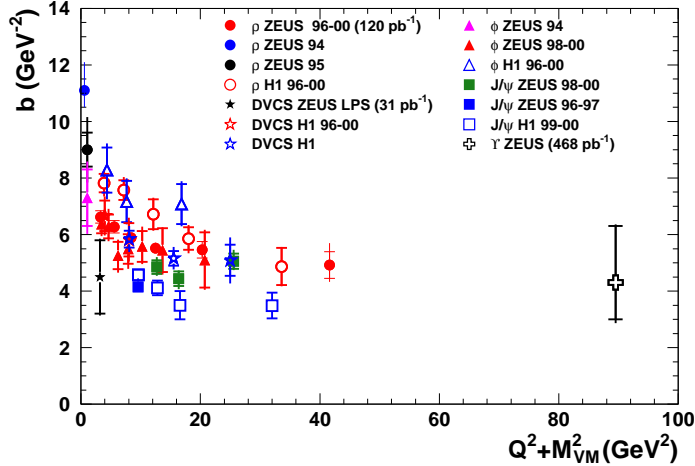


**Figure 8:** The dependence of the slope for DIS processes ( $\sigma_{el}/dt \propto \exp(-Bt)$ ). The picture is taken from Ref. [33].

up to the Tevatron energy. However, we failed to describe the cross sections for diffractive production. Our model gives these cross sections  $\leq 2mb$ . The predictive power of the model is also rather limited. The total inelastic and elastic cross sections are predicted by the model, but the model leads to the value of the slope which is smaller than the TOTEM data. We made a fit in which we include the LHC data in the fitting procedure, to check the stability of our model. This fit is shown by the dashed line in Fig. 3 and Fig. 4. One can see that the difference is very small. Therefore, we can claim that we are not able to describe both the elastic slope and the cross sections for diffractive production.

The parameters that come out from the fit:  $g_s = 0.245$ ,  $\rho = 0.797$  and  $a = 0.23 \text{ GeV}^{-2}$  are large for using  $N = 4$  SYM, in the limit of low  $\rho$ . Therefore the next order correction (at least of the order of  $\rho^2$ ) are needed for a better understanding of the origin of the process of diffractive production in  $N = 4$  SYM.

On the other hand, we cannot avoid the feeling that  $N = 4$  SYM, in the approach of fitting a number of soft observables with only three free parameters, is closely related to the theory of strong interactions at high energies.

We consider this paper as a call for a calculation up to the order of  $\rho^2$  in  $N = 4$  SYM, in which we can find both the source of large mass diffraction, and the correction to the elastic slope.

## Acknowledgments

This work was supported in part by Fondecyt (Chile) grants 1090236 and 1100648.

## References

- [1] E. Gotsman, E. Levin and U. Maor, *Eur. Phys. J. C* **71** (2011) 1553 [arXiv:1010.5323 [hep-ph]].
- [2] A. B. Kaidalov and M. G. Poghosyan, arXiv:0909.5156 [hep-ph].
- [3] A. D. Martin, M. G. Ryskin and V. A. Khoze, arXiv:1110.1973 [hep-ph].
- [4] S. Ostapchenko, *Phys. Rev. D* **83** (2011) 014018 [arXiv:1010.1869 [hep-ph]].
- [5] M. G. Poghosyan, *J. Phys. G* **38**, 124044 (2011) [arXiv:1109.4510 [hep-ex]].
- [6] G. Aad *et al.* [ATLAS Collaboration], *Nature Commun.* **2** (2011) 463 [arXiv:1104.0326 [hep-ex]].
- [7] CMS Physics Analysis Summary: Measurement of the inelastic pp cross section at  $s = 7$  TeV with the CMS detector”, 2011/08/27./
- [8] F. Ferro [TOTEM Collaboration], *AIP Conf. Proc.* **1350** (2011) 172; G. Antchev *et al.* [TOTEM Collaboration], *Europhys. Lett.* **96** (2011) 21002, **95** (2011) 41001 [arXiv:1110.1385 [hep-ex]].
- [9] J. M. Maldacena, *Adv. Theor. Math. Phys.* **2** (1998) 231 [Int. J. Theor. Phys. **38** (1999) 1113] [arXiv:hep-th/9711200]; S. S. Gubser, I. R. Klebanov and A. M. Polyakov, *Phys. Lett. B* **428** (1998) 105 [arXiv:hep-th/9802109]; E. Witten, *Adv. Theor. Math. Phys.* **2** (1998) 505 [arXiv:hep-th/9803131].
- [10] E. Levin and I. Potashnikova, *JHEP* **0906** (2009) 031 [arXiv:0902.3122 [hep-ph]].
- [11] J. Polchinski and M. J. Strassler, *JHEP* **0305** (2003) 012 [arXiv:hep-th/0209211]; *Phys. Rev. Lett.* **88** (2002) 031601 [arXiv:hep-th/0109174].
- [12] Y. Hatta, E. Iancu and A. H. Mueller, *JHEP* **0801** (2008) 026 [arXiv:0710.2148 [hep-th]].
- [13] R. C. Brower, J. Polchinski, M. J. Strassler and C. I. Tan, *JHEP* **0712** (2007) 005 [arXiv:hep-th/0603115].
- [14] R. C. Brower, M. J. Strassler and C. I. Tan, arXiv:0707.2408 [hep-th].
- [15] R. C. Brower, M. J. Strassler and C. I. Tan, *JHEP* **0806** (2008) 048 [arXiv:0801.3002 [hep-th]].
- [16] L. Cornalba and M. S. Costa, *Phys. Rev. D* **78**, (2008) 09010, arXiv:0804.1562 [hep-ph]; L. Cornalba, M. S. Costa and J. Penedones, *JHEP* **0806** (2008) 048 [arXiv:0801.3002 [hep-th]]; *JHEP* **0709** (2007) 037 [arXiv:0707.0120 [hep-th]].
- [17] B. Pire, C. Roiesnel, L. Szymanowski and S. Wallon, *Phys. Lett. B* **670**, 84 (2008) [arXiv:0805.4346 [hep-ph]].
- [18] E. Levin, J. Miller, B. Z. Kopeliovich and I. Schmidt, *JHEP* **0902** (2009) 048; arXiv:0811.3586 [hep-ph].
- [19] E. A. Kuraev, L. N. Lipatov, and F. S. Fadin, *Sov. Phys. JETP* **45**, 199 (1977); Ya. Ya. Balitsky and L. N. Lipatov, *Sov. J. Nucl. Phys.* **28**, 22 (1978).
- [20] M. Froissart, *Phys. Rev.* **123** (1961) 1053; A. Martin, “Scattering Theory: Unitarity, Analyticity and Crossing.” *Lecture Notes in Physics*, Springer-Verlag, Berlin-Heidelberg-New-York, 1969.
- [21] A. Kovner and U. A. Wiedemann, *Phys. Lett. B* **551**, 311 (2003) [hep-ph/0207335] and reference therein.
- [22] A. Karch, E. Katz, D. T. Son and M. A. Stephanov, *Phys. Rev. D* **74** (2006) 015005 [hep-ph/0602229]; H. R. Grigoryan and A. V. Radyushkin, *Phys. Rev. D* **76** (2007) 095007 [arXiv:0706.1543 [hep-ph]].

- [23] S. J. Brodsky and G. F. de Teramond, Phys. Lett. B **582** (2004) 211 [hep-th/0310227]; R. A. Janik and R. B. Peschanski, Nucl. Phys. B **565** (2000) 193 [hep-th/9907177]; H. R. Grigoryan and A. V. Radyushkin, Phys. Rev. D **76** (2007) 095007, [arXiv:0706.1543 [hep-ph]]; P. Colangelo, F. De Fazio, F. Giannuzzi, F. Jugeau and S. Nicotri, Phys. Rev. D **78** (2008) 055009 [arXiv:0807.1054 [hep-ph]]; A. Vega and I. Schmidt, Phys. Rev. D **82** (2010) 115023 [arXiv:1005.3000 [hep-ph]]; A. Vega, I. Schmidt, T. Gutsche and V. E. Lyubovitskij, Phys. Rev. D **83** (2011) 036001 [arXiv:1010.2815 [hep-ph]].
- [24] Z. Abidin and C. E. Carlson, Phys. Rev. D **79** (2009) 115003 [arXiv:0903.4818 [hep-ph]].
- [25] Abramowitz, M. and Stegun, I. A. (Eds.). "Confluent Hypergeometric Functions." Ch. 13 in Handbook of Mathematical Functions with Formulas, Graphs, and Mathematical Tables, 9th printing. New York: Dover, pp. 503-515, 1972.
- [26] K. Nakamura et al. (Particle Data Group), J. Phys. G **37**, 075021 (2010)
- [27] N. A. Amos *et al.* [E710 Collaboration], Phys. Rev. Lett. **68** (1992) 2433.
- [28] J.D. Bjorken, Phys.Rev. D**47** (1993) 101.
- [29] Yuri L. Dokshitzer, Valery A. Khoze, T. Sjostrand, Phys.Lett. B**274** (1992) 116.
- [30] E. Gotsman, E.M. Levin, U. Maor, Phys.Lett. B**309** (1993) 199.
- [31] M. G. Ryskin, A. D. Martin, V. A. Khoze *et al.*, J. Phys. G **G36** (2009) 093001; Eur. Phys. J. **C60** (2009) 265-272; Eur. Phys. J. **C54** (2008) 199 [arXiv:0710.2494 [hep-ph]],
- [32] E. Gotsman, E.M. Levin, U. Maor, Phys. Lett. **B438** (1998) 229; Phys. Rev. **D60** (1999) 094011, [hep-ph/9902294]; E. Gotsman, E. Levin, U. Maor *et al.*, [hep-ph/0511060]; Eur. Phys. J. C **71** (2011) 1685; E. Gotsman, H. Kowalski, E. Levin *et al.*, Eur. Phys. J. **C47** (2006) 655;
- [33] H. Abramowicz *et al.* [ZEUS Collaboration], " *Measurement of the  $t$  dependence in exclusive photoproduction of Upsilon(1S) mesons at HERA,*" arXiv:1111.2133 [hep-ex].